Trends in Chemistry

CellPress

Review

Laser-engraved graphene for flexible and wearable electronics

Minqiang Wang,[1] Yiran Yang,[1] and Wei Gao[1,*]

Laser-engraved graphene (LEG) has been applied increasingly in flexible electronics over the past decade owing to its unique physical and chemical properties, and has shown great promise in energy controls, chemical and physical sensing, and telemedicine. *In situ* laser engraving has empowered graphene with additional versatilities such as miniaturized patterning, tunable composition, controllable morphology, and environmental friendliness. In this review, the technological advances of LEG from synthesis to applications in flexible and wearable electronic devices are summarized. Specifically, the use of LEG in designing next-generation nanogenerators, batteries, supercapacitors, physical sensors, gas sensors, biosensors, and wearable/telemedicine systems is discussed. An outlook related to LEG-based flexible electronics and key technological bottlenecks is identified.

Highlights

Laser engraving allows for versatile and scalable patterning of graphene with various morphologies and electronic properties.

Laser-engraved graphene-based flexible electronic devices show excellent performance in energy control, physical sensing, and analysis of chemical markers in biofluids.

Laser-engraved sensors have been applied in various wearable and telemedicine platforms and have shown great promise in realizing personalized medicine.

The emergence of graphene in flexible electronics

Graphene has been broadly used in the development of flexible electronic devices and systems, thanks to its high theoretical specific surface area, mobility, flexibility, mechanical strength, conductivity, and biocompatibility [1–6]. The fabrication of graphene is commonly achieved by **chemical vapor deposition** (see Glossary), **mechanical exfoliation**, and **wet chemical reduction of graphene oxide** (GO) [7–9]. Although conventional processing techniques, such as screen-printing, roll-to-roll printing, and inkjet printing, have been used to fabricate graphene-based devices [10–12], in most cases, restacking of graphene sheets in the presence of additives hinders their performance [13,14]. An important frontier lies in the large-scale, low-cost production of high-performance and versatile graphene-based electronics for wide-range applications of graphene in consumer devices, and LEG has shown great potential to this end. This article provides an overview of the recent advances in LEG and LEG-based flexible electronics, as illustrated in Figure 1. The *in situ* synthesis and characterization of LEG from precursor substrates are summarized along with the laser reduction of GO. Subsequently, LEG-enabled functionalities toward flexible electronics, including energy control, chemical and physical sensing, and system-level of **telemedicine** are reviewed in detail. Challenges and outlook are discussed for the applications of LEG in personalized healthcare.

Laser-engraved graphene

Laser processing technologies permit scalable patterning of graphene on various substrates, primarily either via laser-induced direct carbonization of polymeric substrates [e.g., polyimide (PI), polyethyleneimine] or laser-induced reduction of GO. Considering that laser engraving plays a crucial role in strategies for both graphene formation and patterning, we categorize all the resulting graphene structures as LEG in this review. UV laser ablation was initially used to pattern carbonized structures on PI film in the 1990s [15]. In the 2010s, it was found that commercially available CO_2 laser cutters could be used to directly engrave and pattern porous graphene on various synthetic and natural carbon precursor (e.g., PI) substrates under ambient conditions

[1]Andrew and Peggy Cherng Department of Medical Engineering, California Institute of Technology, Pasadena, CA 91125, USA

*Correspondence: weigao@caltech.edu (W. Gao).

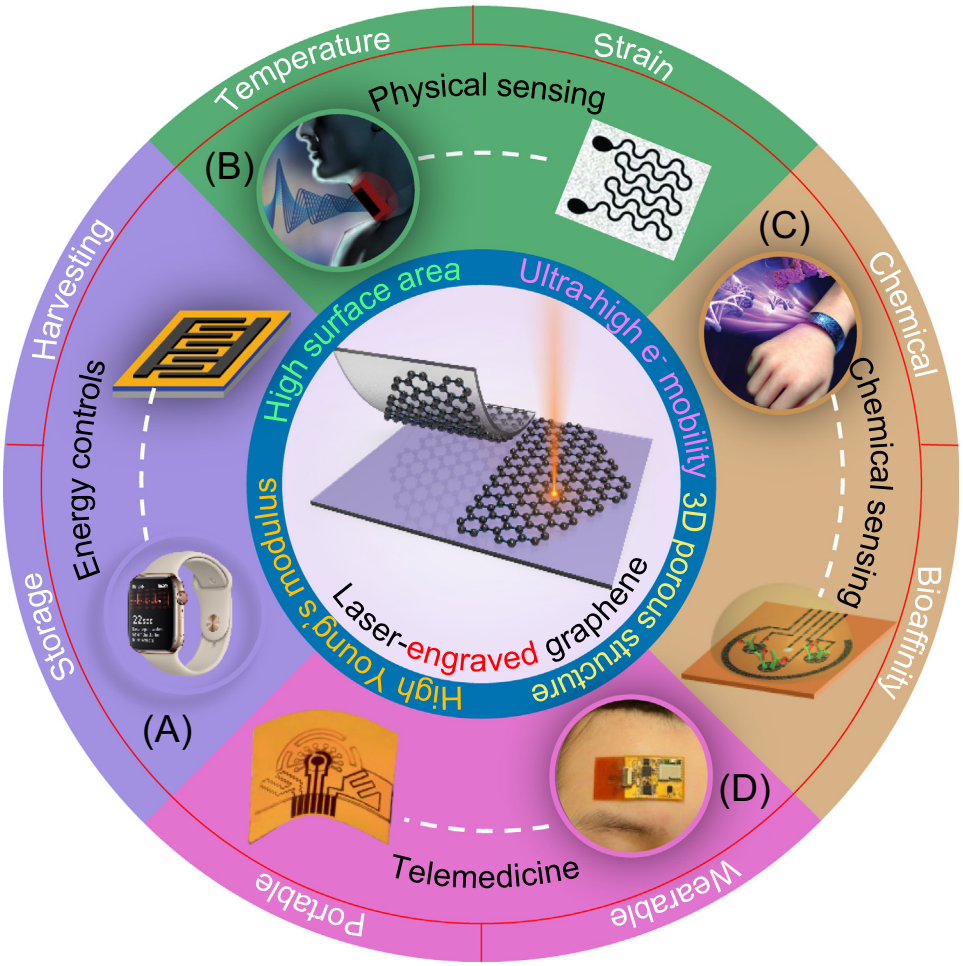

Figure 1. An overview of LEG-based flexible and wearable electronic devices. (A) LEG-based energy control. Adapted, with permission, from [24]. (B) LEG-based physical sensing. Adapted, with permission, from [32,34]. (C) LEG-based chemical sensing. Adapted, with permission, from [31,84]. (D) LEG-based telemedicine. Adapted, with permission, from [30]. Abbreviation: LEG, laser-engraved graphene.

Glossary

Bioaffinity sensor: a biosensing approach that utilizes a bioreceptor for specific recognition of the target analyte.
Chemical vapor deposition: a vacuum deposition method used to produce high-quality, high-performance, solid materials.
Mechanical exfoliation: a top–down approach that requires mechanical energy in order to exfoliate graphite.
Telemedicine: a practice of medicine using technology to deliver care at a distance and allowing remote patient and clinician contact, care, advice, intervention, and monitoring.
Triboelectric nanogenerators (TENGs): devices that convert mechanical energy into electricity using the triboelectric effect.
Wet chemical reduction of graphene oxide: a protocol that utilizes chemical reactions in the solution phase to prepare graphene from a form of graphene oxide.

[16], without generating hazardous wastes [17]. Since then, LEG has shown tremendous potential for flexible electronics applications, as it has unique electrical and chemical properties and allows rapid customizable prototyping on a large scale and at low cost (Table 1) [18–20].

Direct laser engraving

Direct graphene patterning can be achieved with lasers of various wavelengths, spanning from UV to infrared (IR) (Figure 2A) [33]. When the laser beam reaches the precursor of graphene (i.e., PI), graphene forms in a photochemical and/or photothermal process. The photochemical reaction usually appears when a short-wavelength (i.e., UV or blue) laser source is used, as its high photon energy absorbed can directly break chemical bonds and form a dense graphene structure (Figure 2B–D) [33,34]. The photothermal reaction could become predominant when a longer-wavelength (i.e., IR) laser source is used, as the absorbed laser energy is converted into local heat and thus leads to a high localized temperature (>2500°C) [16]. It should be noticed that multiple laser parameters (e.g., wavelength [22,35,36], power [37], pulse width [38], and

Table 1. LEG prepared with different conditions, along with their application[a]

Precursors	Laser source	Parameters (wavelength/pulse duration/intensity)	Applications	Refs
GO	KrF excimer laser	308 nm, 105 mJ cm^{-2}	Supercapacitors	[21]
PI	UV	355 nm, 1 μs, 300 mW	Strain sensing	[22]
Phenolic resin	Visible light	405 nm, 2 μs, 500 mW	Supercapacitors	[23]
GO film	LightScribe DVD optical drive	780 nm, 5 mW	Supercapacitors	[24]
GO	Femtosecond laser	800 nm, 120 fs, 16–60 nJ	Electronic circuits and memory cards	[25]
V_2O_5–GO film	Near-IR laser	1064 nm, 10 μs	Supercapacitor	[26]
Metal-complex-containing polyethersulfone	CO_2 laser	10.6 μm, 40 W	Photoelectrochemical sensing	[27]
Cloth, paper, and food	CO_2 laser	10.6 and 9.3 μm, 75 and 50 W	Supercapacitors	[17]
Kevlar textile	CO_2 laser	10.6 μm, 5.5–8.0 W	Zn–air battery, ECG monitoring, NO_2 sensing	[28]
PI	CO_2 laser	10.6 μm, 14 μs, 2.4–5.4 W	Supercapacitors	[16]
PI	CO_2 laser	10.6 μm, 50 W	COVID-19 diagnosis	[29]
PI	CO_2 laser	10.6 μm, 50 W	Multi-module sweat analysis	[30]
PI	CO_2 laser	10.6 μm, 50 W	Sweat cortisol analysis	[31]
PI	CO_2 laser	10.6 μm, 14 μs, 30 W	EEG, ECG, and EMG monitoring	[32]

[a]Abbreviations: ECG, electrocardiography; EEG, electroencephalography; EMG, electromyography.

scanning speed) play a key role in the final graphene structure formation and should be considered concurrently during graphene fabrication. When engraving the PI with a 10.6-μm CO_2 laser cutter, chemical bonds in the PI network are broken and thermal reorganization of the carbon atoms occurs, resulting in sheets of graphene structures (Figure 2E–G) [30,33]. It has been shown that such LEG flakes are full of defects, expanding a hexagon lattice with two pentagons and one heptagon, which could lead to a porous structure [39]. With custom laser settings, different morphologies of the graphene structure can be directly patterned on PI, ranging from isotropic pores, cellular networks, and nanofibers [37].

Although laser engraving remains a 2D-patterning process, various strategies have been developed to utilize laser engraving to achieve 3D graphene foam of various structures. Laminated object manufacturing was utilized to stack multiple layers of PI-based LEG together and the resulting cubic graphene foam was further carved to the desired shape with fiber laser milling [40]. Furthermore, layer-by-layer CO_2 laser sintering was performed on Ni-sucrose powder which enabled free-standing graphene foam structures with high porosity and electrical conductivity [41].

Laser reduction of GO

GO, prepared by chemical exfoliation of graphite, can be converted into reduced GO (rGO) with defined patterns directly by laser radiation and thus provide feasible strategies for graphene-based electronics. It has rich oxygen-containing groups (OCGs) on the graphene skeleton and has high photon absorption, thanks to its narrowband structures. These OCGs can be cut down through photochemical and photothermal processes easily, even with a weak photon energy laser (Figure 2H) [42]. Under laser thermal reduction, GO undergoes a disproportionation reaction to yield rGO, accompanied by the evolution of carbonaceous gases. Huang and co-workers have described the detailed chemical reactions involved during the thermal reduction of GO [43]. GO nanoflakes can be easily deployed on various substrates and then rGO can be

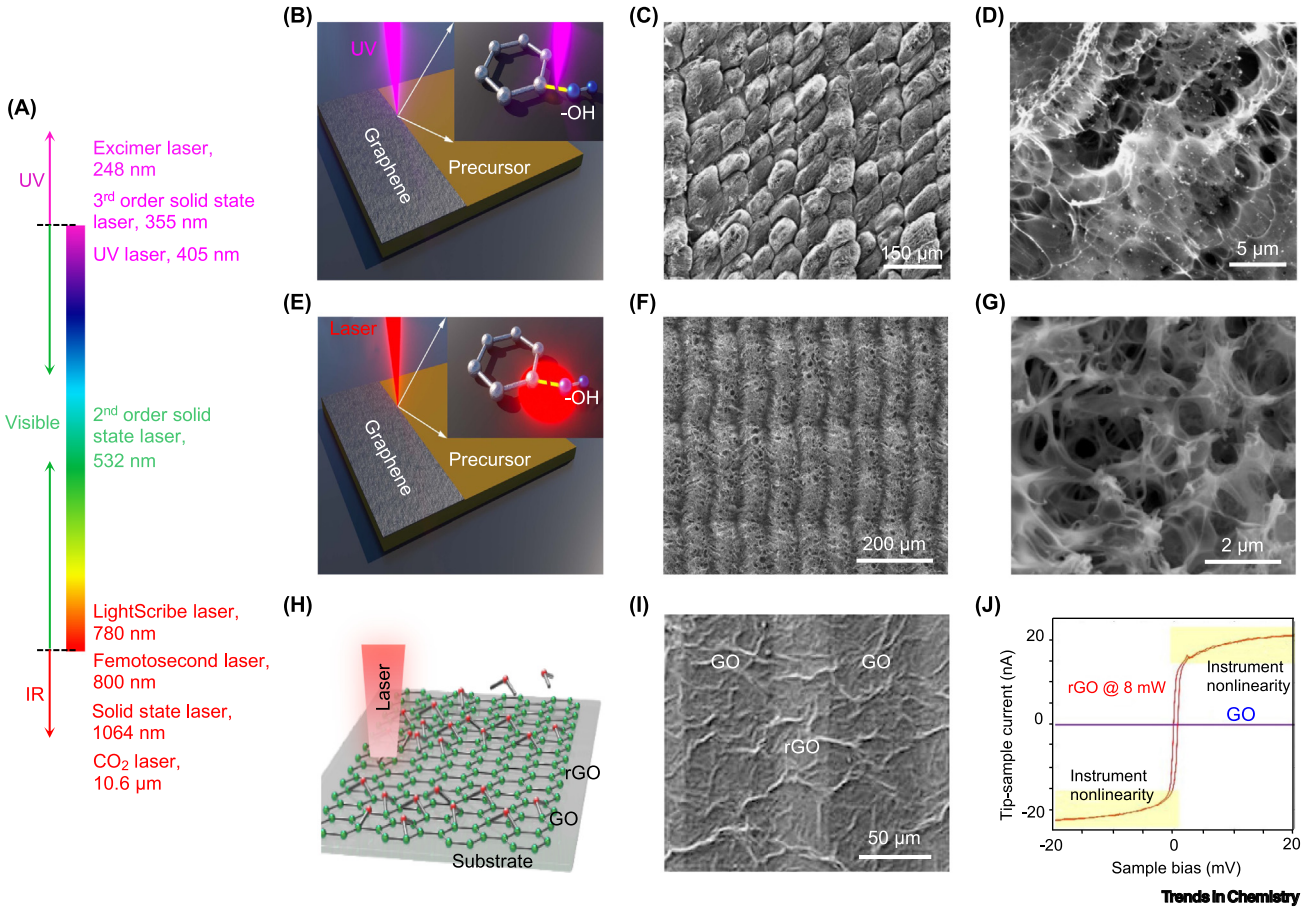

Figure 2. Fabrication and characterization of LEG. (A) Laser sources used for graphene engraving. (B) Schematic of the photochemical process using UV as energy source. Adapted, with permission, from [33]. (C,D) SEM images of LEG on PI produced by a 450-nm laser. Adapted, with permission, from [34]. (E) Schematic of the photothermal reorganization process of LEG from precursor substrates. Adapted, with permission, from [33]. (F,G) SEM image of LEG on PI produced by a CO_2 laser. Adapted, with permission, from [30]. (H) Schematic illustration of the laser reduction of GO to rGO. (I) SEM image of the plane rGO/GO/rGO configuration on the GO film. Adapted, with permission, from [44]. (J) Current-sensing atomic force microscopy current–voltage characteristic (*I–V*) curves of the rGO reduced with an 8-mW laser. Adapted, with permission, from [45].

directly patterned onto the substrate. The rGO microcircuits on a GO film were fabricated in a mask-free manner with 800-nm femtosecond laser reduction; the in-plane rGO/GO/rGO nano-configuration is illustrated in Figure 2I [44]. The degree of reduction and conductivity of the rGO obtained under different laser power settings were investigated using current-sensing atomic force microscopy (CSAFM). As shown in Figure 2J, while the GO film remains insulated, the rGO pattern which is reduced with an 8-mW laser becomes conductive [45]. Laser reduction also results in a 3D hierarchical structure that contributes to the high conductivity and anisotropy of the laser-engraved rGO [46,47].

LEG-based energy control devices

Flexible energy control devices are promising solutions for efficient energy harvesting and storage. Laser processing substantially simplifies the manufacture and integration of graphene structures for flexible energy control. A wide range of LEG-based flexible energy control devices have been developed recently and are summarized below.

LEG-based energy harvesting devices

Triboelectric nanogenerators (**TENGs**) are a highly attractive energy harvesting approach capable of harvesting mechanical energy and converting it into electricity [48,49]. A flexible TENG based on an MXene-polydimethylsiloxane composite film and an LEG electrode was developed (Figure 3A); this TENG, used as a writing board, produces voltage signals based on contact electrification as well as electrostatic induction between two electrodes [50]. LEG was also utilized as high-efficiency TENG electrodes, which produced a significantly higher electrical output compared to adhesive aluminum electrodes [51].

Direct laser patterned rGO was successfully applied in flexible organic photovoltaic (OPV) devices (Figure 3B), which displayed high power conversion efficiency for flexible OPV devices [52]. The optical and electrical properties of rGO micromesh were tuned by controlling the periodicity, irradiation time, and neck width of the mesh, which led to the device possessing unique properties such as excellent flexibility, transparency, and conductivity.

In addition to TENGs and OPVs, LEG has been employed for the development of integrated flexible biofuel cells, as shown in Figure 3C. The LEG-based bioanode and biocathode were modified with glucose dehydrogenase (GDH) and bilirubin oxidase (BOD), respectively. Owing to the high conductivity and electrochemical performance of LEG, the constructed biofuel cell produced a maximum power density of 27 ± 1.7 μW cm^{-2} at an open circuit voltage of 0.45 ± 0.03 V. In addition, the device displayed great mechanical robustness and lifetime [53].

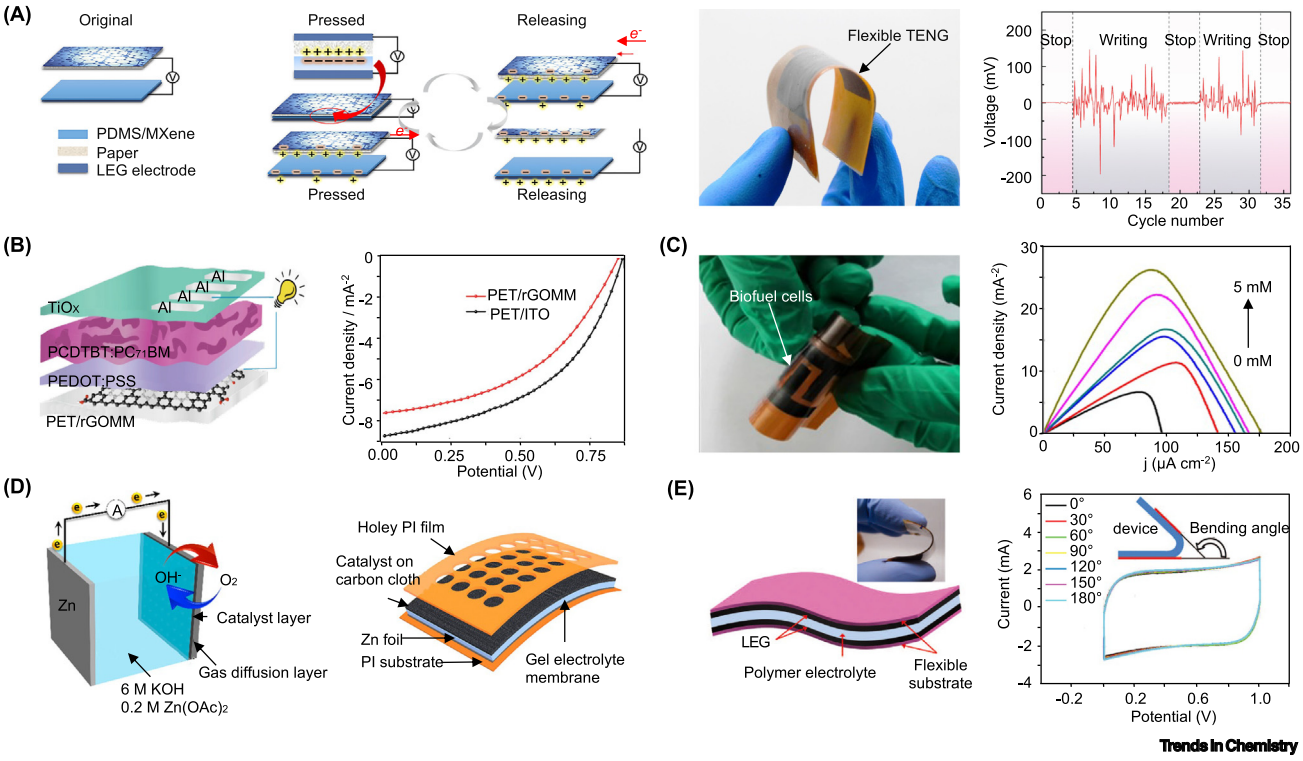

Figure 3. LEG for energy control. (A) An LEG-based TENG writing tablet for writing motion monitoring. Adapted, with permission, from [50]. (B) A BHJ OPV device with LEG as a transparent conductive electrode. Adapted, with permission, from [52]. (C) LEG-based enzymatic glucose biofuel cells. Adapted, with permission, from [53]. (D) LEG-based rechargeable Zn–air battery. Adapted, with permission, from [56]. (E) An all-solid-state LEG-based flexible electrochemical capacitor. Adapted, with permission, from [61]. Abbreviations: BHJ OPV, bulk-heterojunction flexible organic photovoltaic; LEG, laser-engraved graphene; TENG, triboelectric nanogenerator.

LEG-based energy storage devices

LEG has been used for the development of flexible energy storage devices such as rechargeable batteries [54–57]. With an ultrahigh theoretical energy density of 1218 Wh kg^{-1}, Zn–air battery is a promising alternative energy storage device, but there is a pressing need for an inexpensive and efficient cathode [54,55]. Integration of LEG with different nanomaterials can enrich its functionality and offer an attractive approach for preparing a high-performance low-cost battery cathode. As shown in Figure 3D, a ternary metal oxide/LEG hybrid dual oxygen reduction reaction/oxygen evolution reaction catalyst was directly fabricated using CO_2 laser by engraving the precursor (Co, Ni, and Fe ions)-loaded LEG [56]. After assembly of the optimized catalyst cathode with a zinc plate as the anode, a flexible Zn–air battery was prepared that displayed a peak discharge power density of 98.9 mW cm^{-2} and an energy density of 842 Wh kg^{-1}. The introduction of LEG significantly increased the specific surface area and porosity of the catalyst, thereby substantially increasing the catalytic active sites. With a significant reduction in the nucleation barrier of lithium ions, the LEG-based composite material was also applied to improve the coulomb efficiency and capacity degradation of lithium-metal anode [58].

Supercapacitors, which are electrical energy storage devices based on the mechanism of electrical double-layer capacitance, have a typical layout that includes either planar or thin film interdigitated architectures [59]. An in-plane interdigital configuration micro-supercapacitor electrode was patterned directly with laser on GO-coated substrates [60]. Direct laser reduction of GO to rGO on a standard LightScribe DVD optical drive was performed to fabricate in-plane electrodes with excellent electrical conductivity (1738 S m^{-1}) and large surface area (1520 m^2 g^{-1}) [61]. The electrodes can thus be used to fabricate an all-solid-state flexible supercapacitor, which exhibits excellent energy density and stability after 1000 cycles of bending tests (Figure 3E). Scalable fabrication of LEG-micro-supercapacitors on a flexible substrate leads to a very high power density of ~200 W cm^{-3} [24]. Although GO can be developed as a supercapacitor device with great performance, the coating of the GO increases the fabrication complexity. LEG electrodes with a 3D porous structure dramatically enlarge the surface area, which increases the specific capacitance. Because of these benefits, LEG has therefore been widely used to improve the performance of supercapacitors [16,62].

LEG-based physical sensors and gas sensors

Owing to their unique electronic properties, LEG can serve as a great candidate for monitoring the physical parameters (e.g., temperature and strain) and gas molecules by detecting the changes in LEG's electrical properties (e.g., resistance and impendence). In this section, we summarize the mechanism of LEG-based physical and gas sensing toward the physiological monitoring of vital signs.

Temperature and strain sensors

Unique 3D LEG structures with tuned laser parameters can be used for designing temperature or strain sensors [22,32,63–65]. As illustrated in Figure 4A,B, vector mode laser engraving can be used to fabricate microstructures that are sensitive to temperature and strain. By controlling the sensors' layout design and laser settings, the LEG temperature sensor can be designed to be less susceptible to strain variations, while the strain sensor can be optimized to achieve the highest strain response [30]. Increase in temperature can lead to an increase in LEG conductivity due to the enhanced electron–phonon scattering and the electron thermal velocity of electrons in the sandwiched layer (Figure 4A). The LEG-based strain sensors are based on the piezoresistive effect with its ultra-porous structure (Figure 4B); when an external strain is applied, the compressed 3D porous structure of the strain sensor results in a decrease in resistance, which could be further used for accurate monitoring of respiration and heart rates.

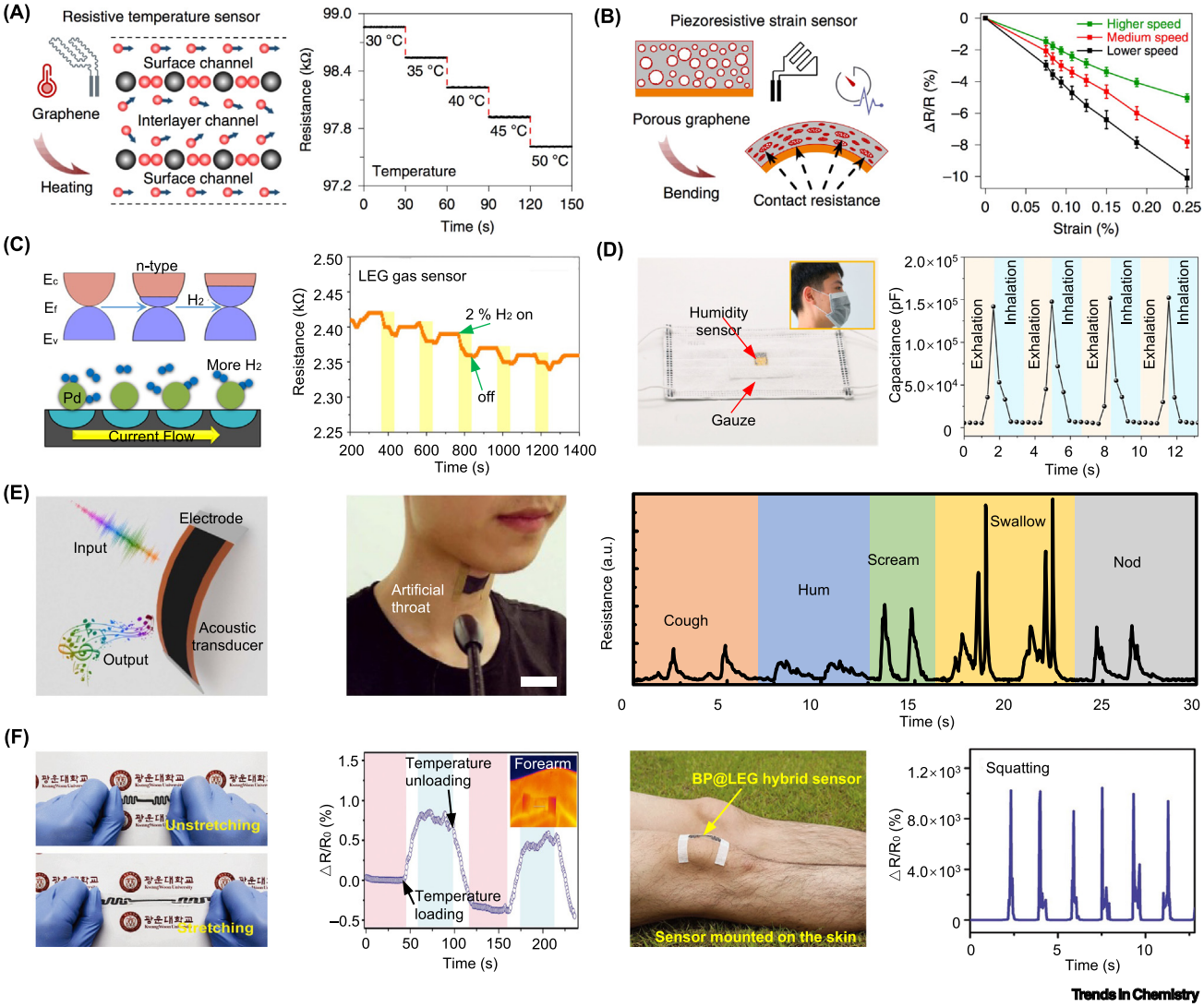

Figure 4. LEG-based physical sensors and gas sensors. (A) Mechanism and dynamic response of an LEG-based temperature sensor. (B) Mechanism and strain responses of LEG-based train sensors. Adapted, with permission, from [30]. (C) An LEG-based H_2 sensor. Adapted, with permission, from [68]. (D) An LEG-based humidity sensor for respiration monitoring. Adapted, with permission, from [69]. (E) An LEG-based artificial throat toward real-time throat vibration monitoring. Adapted, with permission, from [34]. (F) Black phosphorus@LEG heterostructure-based temperature-strain hybrid sensor. Adapted, with permission, from [71]. Abbreviation: LEG, laser-engraved graphene.

Gas and humidity sensors

Laser-treated rGO is attracting more research interest in gas sensing [66]. The adsorption and desorption of gas molecules on the rGO surface change its resistance. An all-graphene flexible NO_2 sensor was developed and used for reversible NO_2 detection via the change in sheet resistance [67]. Although graphene has excellent sensing properties toward polar molecules, it is insensitive to most nonpolar molecules such as H_2. As demonstrated in Figure 4C, through *in situ* laser cutting, noble metal atoms sensitive to H_2 molecules are modified onto the surface of graphene, producing an artificial nose for highly sensitive H_2 detection [68]. In addition to gas molecules, rGO also enables the sensing of humidity due to the strong interaction between OCGs and water molecules. With tuned laser engraving, rGO with different OCG content and

conductivity can be obtained, enabling a high sensitivity for detecting environmental humidity [46]. A flexible humidity sensor with LEG interdigital electrodes and a humidity-sensitive GO film were engraved on a flexible PI substrate for capacitive sensor-based human respiration sensing with high sensitivity, low hysteresis, and long-term stability (Figure 4D) [69].

LEG-based vital sign monitors

Wearable and flexible physiological monitors are able to collect the key vital signs continuously and play a crucial role in personalized healthcare [70]. An LEG artificial throat was fabricated through a photochemical process using a 450-nm laser source (Figure 4E). Various throat vibrations produced by coughs, hums, screams, swallowing, and nods could be monitored by measuring the resulting resistance change in the wearable LEG device [34]. In addition, the integration of the electrical properties of black phosphorus and LEG demonstrated a paradigm for a dual-model temperature- and strain-sensing platform to modulate the e-skin's sensing functionality (Figure 4F) [71]. The excellent physical properties of LEG and LEG composites render excellent performance for detecting many other health-related physical signals, including passive pressure, diastolic and systolic blood pressure, electrocardiogram (ECG), and arterial pulse waveforms [72,73].

LEG-based biosensors

Biosensors, relying on chemical reactions or biorecognition for target molecular detection, provide essential solutions to assess human health at the molecular level. LEG is a promising new candidate in electrochemical biosensors due to its attractive electrochemical properties such as large surface area, excellent stability, and abundant catalytic active sites, which significantly improve the electron transfer kinetics and thereby enable the sensitive detection of biomarkers in biofluids.

Direct molecular detection on the LEG

Benefiting from the rich catalytic active sites induced by the laser engraving process, highly active LEG can directly differentiate and quantify electroactive analytes that have intrinsically distinct oxidation potentials. For example, a flexible LEG chemical sensor for continuous uric acid (UA) and tyrosine (Tyr) monitoring was developed (Figure 5A) [30]. Other electroactive small molecules such as dopamine (DA), epinephrine (EP), norepinephrine (NE), hydrazine, and sodium sulfate could also be detected in this way [74–76]. Functionalization of LEG with metallic nanoparticles endows pristine LEG with increased conductivity and improved sensitivity [77–80]. In addition to direct detection of electroactive molecules, functionalization of LEG with ion-selective membranes realizes real-time monitoring of a variety of ions (e.g., K^+, NH_4^+, Ca^{2+}) via potentiometry [38,81,82]. Using a modified form of polyaniline, a highly stretchable LEG-based potentiometric pH sensor was developed for point-of-care applications [81]. Alternatively, sensitive detection of heavy metal ions was achieved on the LEG with stripping voltammetry that involved deposition of the target metal phase onto the electrode, followed by selective oxidation of the deposited metal film (Figure 5B) [83].

LEG-based bioaffinity sensors

By contrast to direct chemical sensing on LEG, LEG-based **bioaffinity sensors** are established by modifying the LEG surface with 'bioreceptors' such as antibodies, molecularly imprinted polymers (MIPs), and aptamers [84]. The synergistic combination of the conductive LEG and recognition elements (bioreceptors) renders an extraordinary sensing selectivity and sensitivity. As schematically illustrated in Figure 5C, an LEG-based competitive electrochemical immunosensor was developed to monitor the diurnal dynamics of cortisol and stress response in biofluids (serum, saliva, and sweat) [31]. LEG-based label-free electrochemical immunosensors can also

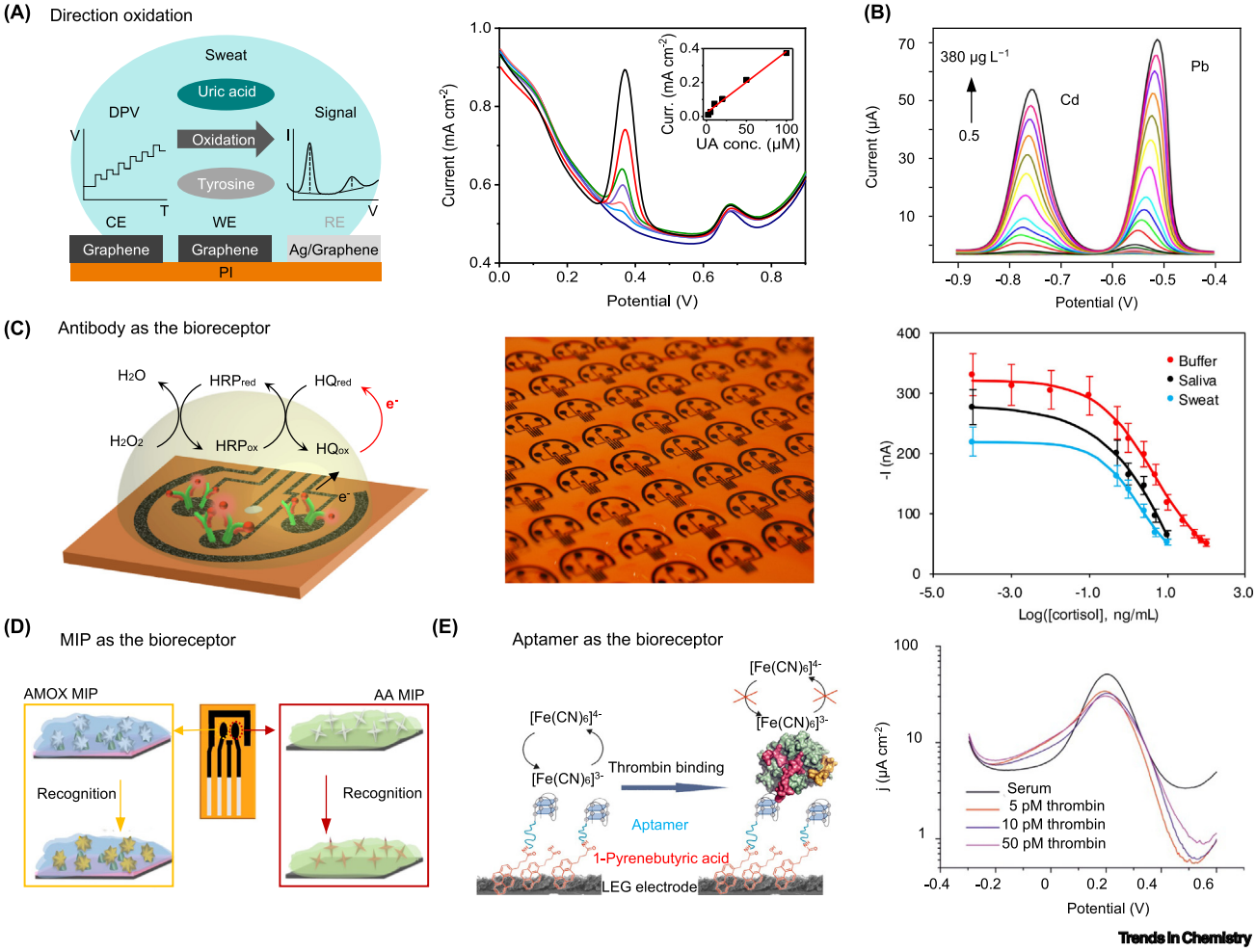

Figure 5. LEG-based biosensors. (A) An LEG-based biosensor for simultaneous UA and Tyr detection. Adapted, with permission, from [30]. (B) Dynamic responses of an LEG-based heavy metal sensor. Adapted, with permission, from [83]. (C) An LEG-based electrochemical immunosensor array for rapid sweat cortisol monitoring. Adapted, with permission, from [31]. (D) An LEG-based dual-MIP sensor for detection of AA and AMOX. Adapted, with permission, from [86]. (E) An LEG-based aptamer sensor for electrochemical thrombin detection. Adapted, with permission, from [87]. Abbreviations: AA, ascorbic acid; AMOX, amoxicillin; LEG, laser-engraved graphene; MIP, molecularly imprinted polymer; Tyr, tyrosine; UA, uric acid.

be designed to detect *Salmonella enterica* without sample preconcentration [85]. Instead of natural antibodies, MIPs have been deemed as biomimetic 'artificial receptors' and display excellent binding selectivity to target molecules. The modifications of MIPs on two conductive LEG working electrodes enabled the highly sensitive detection of amoxicillin and ascorbic acid with great sensitivity and selectivity [86] (Figure 5D). Aptamer, another alternative affinity bioreceptor, was used to functionalize the LEG electrodes for thrombin detection in a redox system; the sensor displayed picomolar sensitivity in the complex matrix of serum (Figure 5E) [87].

LEG for wearable and telemedicine applications

The attractive physical, chemical, and mechanical properties of LEG provide a feasible means for large-scale, low-cost fabrication of wearable and telemedicine sensor patches toward personalized healthcare applications. Transferring or printing LEG fabricated from the PI substrate to a more flexible, stretchable, and gas-permeable substrate allows conformal contact with the skin, enabling high-performance wearable sensing with attractive mechanical resiliency for

monitoring of vital signs [32,88]. A soft and gas-permeable device was fabricated by integrating laser-patterned porous graphene on sugar-templated silicone elastomer sponges (Figure 6A), and the resulting device showed excellent performance in on-body monitoring of electrophysiological signals, temperature, and hydration [32]. Considering that continuous sweat analysis could provide insightful information about an individual's health state at the molecular level [29,89,90], an all-laser-engraved multimodal lab-on-skin was developed, which consisted of LEG-based physical sensors for vital sign monitoring (e.g., temperature, heart rate, and respiration), LEG-based chemical sensors for monitoring of trace-level sweat metabolites and nutrients (e.g., UA and Tyr), and a microfluidic module for efficient sweat sampling (Figure 6B) [30]. This wireless wearable platform was successfully evaluated in a pilot study involving both healthy subjects and gout patients toward noninvasive gout management through real-time, continuous monitoring of sweat UA (Figure 6B) [30]. To combat the coronavirus disease 2019 (COVID-19) pandemic, a fully integrated point-of-care LEG-based multiplex telemedicine platform [severe acute respiratory syndrome–related *coronavirus 2 (*SARS-CoV-2) RapidPlex] was developed for rapid COVID-19 diagnosis and management (Figure 6C). It could simultaneously and quantitatively analyze the virus antigen, virus antibodies, and C-reactive protein in saliva and blood samples from patients with COVID-19, providing information on current infection, infection severity, and immune response [29].

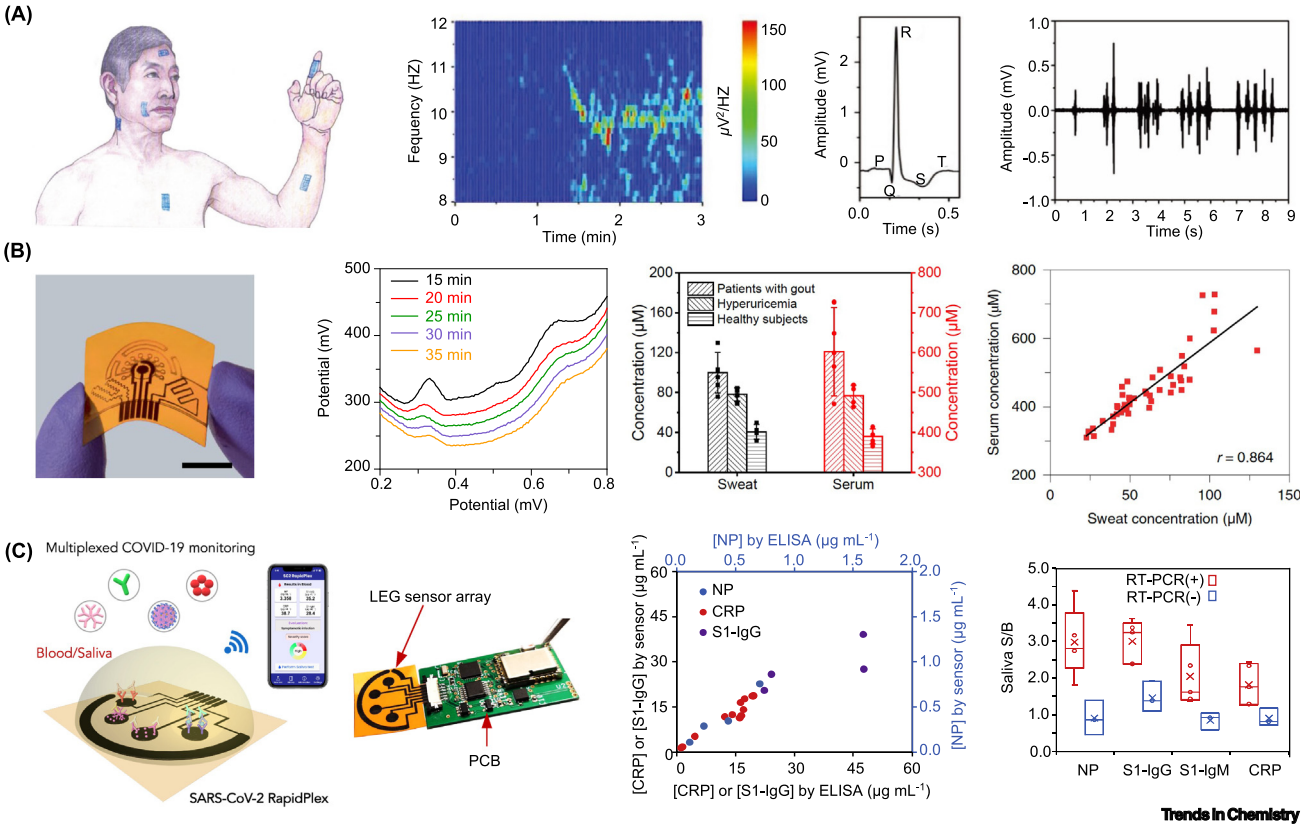

Figure 6. LEG for wearable and telemedicine applications. (A) LEG-based multifunctional devices to monitor electrophysiological activities, including alpha rhythm, ECG, and EMG. Adapted, with permission, from [32]. (B) A flexible all-laser-engraved multimodal wearable patch for the dynamic monitoring of sweat UA toward gout management. Adapted, with permission, from [30]. (C) A multiplexed telemedicine platform SARS-CoV-2 RapidPlex for rapid COVID-19 diagnosis and monitoring. Adapted, with permission, from [29]. Abbreviations: COVID-19, coronavirus disease 2019; ECG, electrocardiogram; EMG, electromyography; LEG, laser-engraved graphene; UA, uric acid.

Concluding remarks

Recent progress in LEG sensors has revealed the versatile use of graphene for energy control, physical sensing, direct chemical sensing, and affinity-based biosensing. Compared with conventional graphene fabrication techniques, the laser engraving process allows simple, mass-producible, and inexpensive graphene patterning in ambient conditions. Various LEG features, including porosity, composition, impedance, and morphology, can be tuned on different laser parameters, rendering the possibility for diverse flexible on-skin electronic devices. The high-biocompatibility, gas-permeability, and antibacterial properties of LEG are also beneficial for its bioelectronics and wearable applications.

Despite the great promise, there are critical challenges to be resolved to realize the full potential of LEG, such as relatively low mobility (compared with vacuum-processed graphene [91]), the mechanical stability of LEG on a flexible substrate, poor stretchability compared with elastomers, and the durability for long-term on-skin use (see Outstanding questions). The electrical and mechanical properties may be potentially improved with strategic polymeric coating or optimization of the laser engraving parameters. *In situ* and *ex situ* modifications on LEG could further enhance its properties, such as electrical conductivity and specificity, in both physical and chemical sensing. Highly stretchable LEG-based electronic devices can be potentially achieved through transfer printing of the patterned LEG onto a soft elastomer substrate. Moreover, although current source materials for direct LEG are mostly based on PI and polyethyleneimine, new material choices are being explored, such as lignin-containing wood [92], sulfonated poly(ether ketone) [93], and phenolic resin [23], which could also potentially shed light on resolving some of the challenges aforementioned. Nonetheless, the diversity of use of LEG has resulted in fruitful applications and with future research endeavors, LEG-based flexible electronics may become commonplace products in future wearables.

Outstanding questions

Will further *in situ* and *ex situ* modifications in engraving workflow substantially improve the mechanical stability, reproducibility, electrical, and electrochemical properties of LEG-based flexible electronic devices?

Will new sensing modalities or strategies allow for LEG-based wearable biosensors to continuously and selectively monitor ultralow levels of biomarkers such as proteins, peptides, hormones, metabolites, and nutrients in body fluids?

What kinds of new applications could LEG-based flexible electronics enable?

How can the translation of LEG-based wearable or telemedicine technologies be realized and accelerated?

Acknowledgments

This project was supported by the Translational Research Institute for Space Health through NASA NNX16AO69A, Office of Naval Research Award N00014-21-1-2483, High Impact Pilot Research Award T31IP1666, and grant R01RG3746 from the Tobacco-Related Disease Research Program.

Declaration of interests

No interests are declared.

References

1. Geim, A.K. (2009) Graphene: status and prospects. *Science* 324, 1530–1534
2. Han, T.-H. *et al.* (2017) Graphene-based flexible electronic devices. *Mater. Sci. Eng. R. Rep.* 118, 1–43
3. Kim, S.J. *et al.* (2015) Materials for flexible, stretchable electronics: graphene and 2D materials. *Annu. Rev. Mater. Res.* 45, 63–84
4. Zhang, Z. *et al.* (2017) Rosin-enabled ultraclean and damage-free transfer of graphene for large-area flexible organic light-emitting diodes. *Nat. Commun.* 8, 14560
5. You, R. *et al.* (2020) Laser fabrication of graphene-based flexible electronics. *Adv. Mater.* 32, e1901981
6. Khan, U. *et al.* (2017) Graphene tribotronics for electronic skin and touch screen applications. *Adv. Mater.* 29, 1603544
7. Chen, Z. *et al.* (2011) Three-dimensional flexible and conductive interconnected graphene networks grown by chemical vapour deposition. *Nat. Mater.* 10, 424–428
8. Xu, Y. *et al.* (2010) Self-assembled graphene hydrogel via a one-step hydrothermal process. *ACS Nano* 4, 4324–4330
9. Eigler, S. *et al.* (2013) Wet chemical synthesis of graphene. *Adv. Mater.* 25, 3583–3587
10. Bae, S. *et al.* (2010) Roll-to-roll production of 30-inch graphene films for transparent electrodes. *Nat. Nanotechnol.* 5, 574
11. Hyun, W.J. *et al.* (2015) High-resolution patterning of graphene by screen printing with a silicon stencil for highly flexible printed electronics. *Adv. Mater.* 27, 109–115
12. Capasso, A. *et al.* (2015) Ink-jet printing of graphene for flexible electronics: an environmentally-friendly approach. *Solid State Commun.* 224, 53–63
13. Zhang, Y. *et al.* (2012) Glass carbon electrode modified with horseradish peroxidase immobilized on partially reduced graphene oxide for detecting phenolic compounds. *J. Electroanal. Chem.* 681, 49–55
14. Wang, F. *et al.* (2014) A simple, rapid and green method based on pulsed potentiostatic electrodeposition of reduced graphene oxide on glass carbon electrode for sensitive voltammetric detection of sophoridine. *Electrochim. Acta* 141, 82–88
15. Srinivasan, R. *et al.* (1995) Chemical transformations of the polyimide Kapton brought about by ultraviolet laser radiation. *J. Appl. Phys.* 78, 4881–4887
16. Lin, J. *et al.* (2014) Laser-induced porous graphene films from commercial polymers. *Nat. Commun.* 5, 5714
17. Chyan, Y. *et al.* (2018) Laser-induced graphene by multiple lasing: toward electronics on cloth, paper, and food. *ACS Nano* 12, 2176–2183
18. Ye, R. *et al.* (2018) Laser-induced graphene. *Acc. Chem. Res.* 51, 1609–1620

19. Ye, R. *et al.* (2019) Laser-induced graphene: from discovery to translation. *Adv. Mater.* 31, 1803621
20. Luong, D.X. *et al.* (2019) Laser-induced graphene composites as multifunctional surfaces. *ACS Nano* 13, 2579–2586
21. Hosseini, S.M. *et al.* (2018) Excimer laser assisted very fast exfoliation and reduction of graphite oxide at room temperature under air ambient for Supercapacitors electrode. *Appl. Surf. Sci.* 427, 507–516
22. Carvalho, A.F. *et al.* (2018) Laser-induced graphene strain sensors produced by ultraviolet irradiation of polyimide. *Adv. Funct. Mater.* 28, 1805271
23. Zhang, Z. *et al.* (2018) Visible light laser-induced graphene from phenolic resin: a new approach for directly writing graphene-based electrochemical devices on various substrates. *Carbon* 127, 287–296
24. El-Kady, M.F. and Kaner, R.B. (2013) Scalable fabrication of high-power graphene micro-supercapacitors for flexible and on-chip energy storage. *Nat. Commun.* 4, 1475
25. Liang, J. *et al.* (2010) Toward all-carbon electronics: fabrication of graphene-based flexible electronic circuits and memory cards using maskless laser direct writing. *ACS Appl. Mater. Inter.* 2, 3310–3317
26. Zhang, L.-F. *et al.* (2017) A laser irradiation synthesis of strongly-coupled VOx-reduced graphene oxide composites as enhanced performance supercapacitor electrodes. *Mater. Today Energy* 5, 222–229
27. Ge, L. *et al.* (2019) Direct-laser-writing of metal sulfide-graphene nanocomposite photoelectrode toward sensitive photoelectrochemical sensing. *Adv. Funct. Mater.* 29, 1904000
28. Wang, H. *et al.* (2020) Laser writing of janus graphene/kevlar textile for intelligent protective clothing. *ACS Nano* 14, 3219–3226
29. Torrente-Rodríguez, R.M. *et al.* (2020) SARS-CoV-2 RapidPlex: a graphene-based multiplexed telemedicine platform for rapid and low-cost COVID-19 diagnosis and monitoring. *Matter* 3, 1981–1998
30. Yang, Y. *et al.* (2020) A laser-engraved wearable sensor for sensitive detection of uric acid and tyrosine in sweat. *Nat. Biotechnol.* 38, 217–224
31. Torrente-Rodríguez, R.M. *et al.* (2020) Investigation of cortisol dynamics in human sweat using a graphene-based wireless mHealth system. *Matter* 2, 921–937
32. Sun, B. *et al.* (2018) Gas-permeable, multifunctional on-skin electronics based on laser-induced porous graphene and sugar-templated elastomer sponges. *Adv. Mater.* 30, 1804327
33. Li, G. (2020) Direct laser writing of graphene electrodes. *J. Appl. Phys.* 127, 010901
34. Tao, L.-Q. *et al.* (2017) An intelligent artificial throat with sound-sensing ability based on laser induced graphene. *Nat. Commun.* 8, 14579
35. Duy, L.X. *et al.* (2018) Laser-induced graphene fibers. *Carbon* 126, 472–479
36. Wang, L. *et al.* (2020) A comparative study of laser-induced graphene by CO_2 infrared laser and 355 nm ultraviolet (UV) laser. *Micromachines* 11, 1094
37. Abdulhafez, M. *et al.* (2021) Fluence-dependent morphological transitions in laser-induced graphene electrodes on polyimide substrates for flexible devices. *ACS Appl. Nano Mater.* 4, 2973–2986
38. Garland, N.T. *et al.* (2018) Flexible laser-induced graphene for nitrogen sensing in soil. *ACS Appl. Mater. Inter.* 10, 39124–39133
39. Ma, J. *et al.* (2009) Stone-Wales defects in graphene and other planar s p 2-bonded materials. *Phys. Rev. B* 80, 033407
40. Luong, D.X. *et al.* (2018) Laminated object manufacturing of 3D-printed laser-induced graphene foams. *Adv. Mater.* 30, 1707416
41. Sha, J. *et al.* (2017) Three-dimensional printed graphene foams. *ACS Nano* 11, 6860–6867
42. Liu, Y.Q. *et al.* (2016) Surface and interface engineering of graphene oxide films by controllable photoreduction. *Chem. Rec.* 16, 1244–1255
43. Klemeyer, L. *et al.* (2021) Geometry-dependent thermal reduction of graphene oxide solid. *ACS Mater. Lett.* 3, 511–515
44. Cheng, H. *et al.* (2018) Flexible in-plane graphene oxide moisture-electric converter for touchless interactive panel. *Nano Energy* 45, 37–43
45. Ma, B. *et al.* (2019) The correlation between electrical conductivity and second-order Raman modes of laser-reduced graphene oxide. *Phys. Chem. Chem. Phys.* 21, 10125–10134
46. Guo, L. *et al.* (2012) Two-beam-laser interference mediated reduction, patterning and nanostructuring of graphene oxide for the production of a flexible humidity sensing device. *Carbon* 50, 1667–1673.47
47. Jiang, H.B. *et al.* (2014) Bioinspired fabrication of superhydrophobic graphene films by two-beam laser interference. *Adv. Funct. Mater.* 24, 4595–4602
48. Wang, Z.L. *et al.* (2015) Progress in triboelectric nanogenerators as a new energy technology and self-powered sensors. *Energy Environ. Sci.* 8, 2250–2282
49. Zou, Y. *et al.* (2020) Wearable triboelectric nanogenerators for biomechanical energy harvesting. *Nano Energy* 77, 105303
50. Jiang, C. *et al.* (2019) A multifunctional and highly flexible triboelectric nanogenerator based on MXene-enabled porous film integrated with laser-induced graphene electrode. *Nano Energy* 66, 104121
51. Zhao, P. *et al.* (2020) Replacing the metal electrodes in triboelectric nanogenerators: High-performance laser-induced graphene electrodes. *Nano Energy* 75, 104958
52. Konios, D. *et al.* (2015) Reduced graphene oxide micromesh electrodes for large area, flexible, organic photovoltaic devices. *Adv. Funct. Mater.* 25, 2213–2221
53. Kong, X. *et al.* (2020) Laser-scribed N-doped graphene for integrated flexible enzymatic biofuel cells. *ACS Sustain. Chem. Eng.* 8, 12437–12442
54. Lee, J.S. *et al.* (2011) Metal–air batteries with high energy density: Li–air versus Zn–air. *Adv. Energy Mater.* 1, 34–50
55. Wang, M.-Q. *et al.* (2018) Synthesis of M (Fe_3C, Co, Ni)-porous carbon frameworks as high-efficient ORR catalysts. *Energy Storage Mater.* 11, 112–117
56. Ren, M. *et al.* (2019) Laser-induced graphene hybrid catalysts for rechargeable Zn-air batteries. *ACS Appl. Energy Mater.* 2, 1460–1468
57. Zhang, F. *et al.* (2018) Highly doped 3D graphene Na-ion battery anode by laser scribing polyimide films in nitrogen ambient. *Adv. Energy Mater.* 8, 1800353
58. Yi, J. *et al.* (2019) Facile patterning of laser-induced graphene with tailored Li nucleation kinetics for stable lithium-metal batteries. *Adv. Energy Mater.* 9, 1901796
59. Wang, Y. *et al.* (2009) Supercapacitor devices based on graphene materials. *J. Phys. Chem. C* 113, 13103–13107
60. Gao, W. *et al.* (2011) Direct laser writing of micro-supercapacitors on hydrated graphite oxide films. *Nat. Nanotechnol.* 6, 496–500
61. El-Kady, M.F. *et al.* (2012) Laser scribing of high-performance and flexible graphene-based electrochemical capacitors. *Science* 335, 1326–1330
62. Song, W. *et al.* (2018) Flexible, stretchable, and transparent planar microsupercapacitors based on 3D porous laser-induced graphene. *Small* 14, 1702249
63. Rahimi, R. *et al.* (2015) Highly stretchable and sensitive unidirectional strain sensor via laser carbonization. *ACS Appl. Mater. Inter.* 7, 4463–4470
64. Yang, W. *et al.* (2019) Fabrication of smart components by 3D printing and laser-scribing technologies. *ACS Appl. Mater. Inter.* 12, 3928–3935
65. Bobinger, M.R. *et al.* (2019) Flexible and robust laser-induced graphene heaters photothermally scribed on bare polyimide substrates. *Carbon* 144, 116–126
66. Toda, K. *et al.* (2015) Recent progress in applications of graphene oxide for gas sensing: a review. *Anal. Chim. Acta* 878, 43–53
67. Strong, V. *et al.* (2012) Patterning and electronic tuning of laser scribed graphene for flexible all-carbon devices. *ACS Nano* 6, 1395–1403
68. Zhu, J. *et al.* (2019) Biomimetic turbinate-like artificial nose for hydrogen detection based on 3D porous laser-induced graphene. *ACS Appl. Mater. Inter.* 11, 24386–24394
69. Lan, L. *et al.* (2020) One-step and large-scale fabrication of flexible and wearable humidity sensor based on laser-induced graphene for real-time tracking of plant transpiration at bio-interface. *Biosens. Bioelectron.* 165, 112360

70. Xu, C. *et al.* (2020) Skin-interfaced sensors in digital medicine: from materials to applications. *Matter* 2, 1414–1445
71. Chhetry, A. *et al.* (2020) Black phosphorus@laser-engraved graphene heterostructure-based temperature–strain hybridized sensor for electronic-skin applications. *Adv. Funct. Mater.* 31, 2007661
72. Rahimi, R. *et al.* (2016) Direct laser writing of porous-carbon/silver nanocomposite for flexible electronics. *ACS Appl. Mater. Inter.* 8, 16907–16913
73. Xu, Y. *et al.* (2020) Multiscale porous elastomer substrates for multifunctional on-skin electronics with passive-cooling capabilities. *Proc. Natl. Acad. Sci. U. S. A.* 117, 205–213
74. Xu, G. *et al.* (2018) Detection of neurotransmitters by three-dimensional laser-scribed graphene grass electrodes. *ACS Appl. Mater. Inter.* 10, 42136–42145
75. Han, T. *et al.* (2019) Multifunctional flexible sensor based on laser-induced graphene. *Sensors* 19, 3477
76. Sharma, S. *et al.* (2020) Laser induced flexible graphene electrodes for electrochemical sensing of hydrazine. *Mater. Lett.* 262, 127150
77. Nayak, P. *et al.* (2016) Highly efficient laser scribed graphene electrodes for on-chip electrochemical sensing applications. *Adv. Electron. Mater.* 2, 1600185
78. Aparicio-Martínez, E. *et al.* (2019) Flexible electrochemical sensor based on laser scribed graphene/Ag nanoparticles for non-enzymatic hydrogen peroxide detection. *Sens. Actuators B Chem.* 301, 127101
79. Xuan, X. *et al.* (2018) A highly stretchable and conductive 3D porous graphene metal nanocomposite based electrochemical-physiological hybrid biosensor. *Biosens. Bioelectron.* 120, 160–167
80. Yu, Y. *et al.* (2018) Laser-induced carbon-based smart flexible sensor array for multiflavors detection. *ACS Appl. Mater. Inter.* 10, 34005–34012
81. Rahimi, R. *et al.* (2017) Highly stretchable potentiometric pH sensor fabricated via laser carbonization and machining of carbon–polyaniline composite. *ACS Appl. Mater. Inter.* 9, 9015–9023
82. Kucherenko, I.S. *et al.* (2020) Ion-selective sensors based on laser-induced graphene for evaluating human hydration levels using urine samples. *Adv. Mater. Technol.* 5, 1901037
83. Lin, X. *et al.* (2018) Laser engraved nitrogen-doped graphene sensor for the simultaneous determination of Cd (II) and Pb (II). *J. Electroanal. Chem.* 828, 41–49
84. Tu, J. *et al.* (2020) The era of digital health: a review of portable and wearable affinity biosensors. *Adv. Funct. Mater.* 30, 1906713
85. Soares, R.R. *et al.* (2020) Laser-induced graphene electrochemical immunosensors for rapid and label-free monitoring of *Salmonella enterica* in chicken broth. *ACS Sens.* 5, 1900–1911
86. Marques, A.C. *et al.* (2020) Laser-induced graphene-based platforms for dual biorecognition of molecules. *ACS Appl. Nano Mater.* 3, 2795–2803
87. Fenzl, C. *et al.* (2017) Laser-scribed graphene electrodes for aptamer-based biosensing. *ACS Sens.* 2, 616–620
88. Tehrani, F. *et al.* (2019) Laser-induced graphene composites for printed, stretchable, and wearable electronics. *Adv. Mater. Technol.* 4, 1900162
89. Gao, W. *et al.* (2016) Fully integrated wearable sensor arrays for multiplexed in situ perspiration analysis. *Nature* 529, 509–514
90. Yang, Y. and Gao, W. (2019) Wearable and flexible electronics for continuous molecular monitoring. *Chem. Soc. Rev.* 48, 1465–1491
91. Bhaumik, A. *et al.* (2017) Reduced graphene oxide thin films with very large charge carrier mobility using pulsed laser deposition. *J. Mater. Sci. Eng.* 6, 1000364
92. Ye, R. *et al.* (2017) Laser-induced graphene formation on wood. *Adv. Mater.* 29, 1702211
93. Zhu, C. *et al.* (2019) Direct laser writing of graphene films from a polyether ether ketone precursor. *J. Mater. Sci.* 54, 4192–4201